Nondermal irritating hyperosmotic nanoemulsions reduce treatment times in a contamination model of wound healing

Sean Connell, PhD[1]; Jianming Li, PhD[1,2]; Abigail Durkes, DMV, PhD[4]; Mohammed Zaroura[5]; Riyi Shi[3,6]

1. Medtric Biotech, LLC, West Lafayette, Indiana,
2. Center for Paralysis Research, Purdue University,
3. Department of Basic Medical Sciences, College of Veterinary Medicine, Purdue University,
4. Comparative Pathobiology Department, College of Veterinary Medicine, Purdue University,
5. MorNuco Inc,
6. Weldon School of Biomedical Engineering, College of Engineering, Purdue University, West Lafayette, Indiana

Reprint requests:
Jianming Li, Center for Paralysis
Research, Purdue University, Medtric
Biotech, LLC, 3000 Kent Ave. Suite
D1-104, West Lafayette, Indiana 47907,
United States of America.
Tel: +1 76549 62903;
Fax: +1 76549 47605;
Email: jianming@purdue.edu

ABSTRACT

Increased microbial burden within the wound often complicates wound healing and may lead to subsequent infection or delayed healing. Here, we investigate a novel topical for addressing wound contamination that utilizes hyperosmotic saccharides with a cell membrane disrupting emulsion. These hyperosmotic nanoemulsions (HNE) were administered topically in a full-thickness biopsy model of wound healing. Results show that HNE were well tolerated in noninfected animals with no indications of dermal irritation or acute toxicity. Additionally, HNE was able to reduce bacterial bioburden (*Escherichia coli* and *Enterococcus faecalis*) levels by 3 logs within 24 h when wounds were inoculated with 5×10^6 total CFU. These bactericidal values were similar to wounds treated with silver sulfadiazine. Wound closure showed HNE wounds closed in 7.6 ± 0.2 days while SSD and control required 10.2 ± 0.4 and 10.4 ± 0.3 days, respectively. HNE maintained a moist wound environment, were well debrided, and exhibited improved hemostatic response. Further histological examination revealed enhanced granulation tissue as compared to silver sulfadiazine and control cohorts. These results were corroborated with 3D topographical imprints of the wounds at day 14 which qualitatively showed a smoother surface. In contrast, silver sulfadiazine appeared to delay wound closure. Finally, dermal sensitization and irritation studies conducted in guinea pig and rabbits did not reveal any acute dermal side effects from HNE exposure. The cumulative data indicates nonantibiotic-based HNEs may be a promising topical treatment for the management of contaminated wounds.

Damage to the skin disturbs the protective barrier and exposes the body to microbial contamination. In the event of an infection, the prolonged inflammatory response increases trauma and prevents restoration by inhibiting wound healing. Complications lead to increased morbidity that requires complex management practices with higher treatment costs.

While wound management practices vary by region, antibiotics are often employed to treat infected wounds. Unfortunately, antibiotic misuse has increased the incidence of drug resistance, a problem that continues to undermine the effectiveness of standard antibiotics. Alternative topicals include biocides such as peroxides, iodine, chlorhexidine derivatives, and ionic silver. The majority of these compounds are antiseptics, however, and prolonged exposure has been shown to inhibit the biological processes involved in wound healing. For example, recent evidence has suggested silver-sulfadiazine is cytotoxic toward fibroblasts and keratinocytes, critical components involved in wound healing.[1–4] Further, oxidizing species such as hydrogen peroxide can lead to excess scar formation by initiating the production of proinflammatory mediators. Current treatments are limited in application as the antimicrobial benefits must be balanced with side effects.

Recently, there has been a growing interest in the use of nonionic hyperosmotic saccharides as topical agents in wound management. For example, application of sugars and honeys has been shown to be effective in a variety of injury modalities ranging from postoperative wounds and burns to diabetic ulcers.[5] Hyperosmotic agents are purported to benefit wound healing by creating a bacteriostatic environment and increase microcirculation at the tissue level.[6–8] Specifically, the hyperosmolarity reduce bioburden by dehydrating pathogens. Reduction of intracellular water content stalls DNA synthesis and replication in a variety of bacterial strains. However, through adaptive physiologic mechanisms, certain strains such as *Staphylococcus aureus* remain viable even at osmolarities approaching the solute saturation limit.[9,10]

We previously postulated that osmotic mediated dehydration can be amplified by disrupting the protective cell membrane. We provided formal evidence that a surfactant in concert with hyperosmotic stress induced synergistic

wide spectrum bactericidal action.[11] In particular, these hyperosmotic nanoemulsions (HNE) were composed of a thymol nanoemulsion suspended in a nonionic hyperosmotic matrix of monosaccharides. The work demonstrated the nanoemulsion damaged the cellular membrane and amplified the leakage of intracellular contents in the presence of an osmotic gradient.

To further explore HNE as topical antimicrobial agents, our goal was to evaluate the safety and efficacy of HNE in a full-thickness dermal injury model in rodents. HNE safety was initially assessed using noninfected wounds while in follow-up studies, the wounds were contaminated with a mixture of *Escherichia coli* and *Enterococcus faecalis*. Wound healing was quantified with several metrics including wound planimetry, wound cultures, measurement of wound bed color, surface topology, and histological examination. Controls included standard gauze dressings and a commercially available silver-sulfadiazine cream. Finally, to assess possible dermal side effects, additional sensitization and irritation studies were conducted in rodents and rabbits using U.S. EPA guidelines. Experimental results demonstrate proof of concept and implementation of HNE as a possible treatment candidate for acute wound management.

MATERIALS AND METHODS

Wound dressings

Absorbent cotton gauze pads and silver-sulfadiazine (SSD: PAR Pharmaceuticals, Woodcliff Lake, NJ) cream served as comparative controls. The HNE-based gel was created by heating (60 °C) a 1% (w/w) solution of thymol (Sigma-Aldrich, St. Louis, MO) in distilled water and sonicating to form a uniform dispersion.[11] The suspension was then diluted 20-fold in distilled water and combined with 45 g of finely ground sucrose (Sigma-Aldrich, St. Louis, MO), 45 g of fructose powder (Sigma-Aldrich), and 3 g of commercial grade petrolatum (Unilever, Rotterdam, The Netherlands) to increase viscosity. The final mixtures were stored in sterile 60 mL syringe tubes prior to use.

Preparation of bacterial inoculum

E. coli ATCC 8739 and *E. faecalis* ATCC 29212 (ATCC—Manassas, VA) were used to inoculate wounds in the contamination animal cohorts. The microbes were cultured in Mueller–Hinton II cation-adjusted broth (TekNova, Hollister, CA) and incubated at 37 °C prior to inoculation. Both microbial suspensions were adjusted to an approximate density of 1.0×10^8 CFU·mL^{-1} as determined by McFarland standards using a spectrophotometer (Lambda 25 Spectrophotometer, Perkin Elmer, Waltham, MA) at 600 nm. The final inoculum comprised 0.5 mL of both the *E. coli* and *E. faecalis* suspension in ∼1:1 combination. The inoculum was delivered to the infected group approximately 60 min after insult as a 50 μL aliquot (or 5.0×10^6 total CFU) by a sterile pipette to the center of the open wound and dispersed with a sterile inoculum loop. The aliquot was allowed to air dry at room temperature (25 °C) for another 60 min to allow cellular adhesion before applying the designated treatment and covering with the bandages.

Wound healing model

Adult female guinea pigs (≈400 g) were used for the study. Guinea pigs were housed with a single cage mate, provided food and water ad libitum and maintained on a 12 h light-to-dark cycle in a facility held at room temperature (23 °C). The guinea pigs were maintained according to the regulations of the Laboratory Animal Welfare Act and the studies were approved by the Purdue University Animal Care and Use Committee. Full-thickness dermal injuries of anesthetized adult female guinea pigs were performed using a standard excisional biopsy procedure. Briefly, guinea pigs were anesthetized with an intramuscular injection of a ketamine–xylazine–acepromazine cocktail (60–10–0.6 mg/kg body weight, respectively). The dorsal hair was groomed with clippers and then shaved with a razor blade. An 8 mm diameter sterile biopsy punch was used to create two full-thickness dermal injuries on opposing sides of the dorsal surface on each guinea pig. The biopsy did not penetrate the panniculus carnosus layer. Following insult, the animals were randomly divided into two groups: (i) noninfected and (ii) infected. The noninfected group consisted of 9 animals, with $n = 9$ each for the cotton gauze and HNE treatment. These animals were sacrificed at day 14. The infected group consisted of a 34 total animals. Four of the 34 animals were sacrificed at day 2 ($n = 4$ for HNE and SSD; $n = 8$ for control) and 3 more sacrificed at day 7 ($n = 3$ for HNE and SSD; $n = 6$ for control). The remaining 27 animals were harvested at day 14 ($n = 22$ for HNE, $n = 11$ for SSD, $n = 21$ for control). For all subjects, the injury sites were randomly designated as gauze control, SSD, or HNE. All treatments were covered with an absorbent polyurethane foam pad (Xtrasorb, Derma Sciences, Princeton, NJ) and occlusive dressing (Tegaderm Film, 3M, St. Paul, MN) and secured in place with adhesive retention tape (HypaFix® - Smith and Nephew, Inc., St. Petersburg, FL). Control gauze pads did not receive the foam padding as the cotton provided absorbency. Bandages were changed daily in all cases until complete wound closure. Experimental methods and results for dermal sensitization and irritation studies can be found in Supporting Information, Section A1.

Wound bed morphometrics

Tissue morphometrics were acquired daily until sacrifice point to monitor wound closure. Rate of closure over time was measured through laser assisted planimetry (Silhouette mobile scanner, Aranz Medical, Christchurch, New Zealand) to provide an accurate, reproducible and user-independent means of tracking wound boundaries.[12–14] Rate of closure was reported as percent wound contraction using the following: Wound contraction (%) = $(A_0 - A_t)/A_0 \times 100$, where A_0 is the original wound area ($t = 0$) and A_t is the area of wound at the time of the measurement.

Wound bed color

Wound bed color was measured as an indirect, noninvasive means to assess changes in tissue inflammation. The color was measured with a tricolor stimulus chroma meter (CR-200, Minolta, Osaka, Japan) and the values reported in the CIE $L^*a^*b^*$ color space. The coordinate systems represents luminosity (L^*) and chromaticity (hue) values that
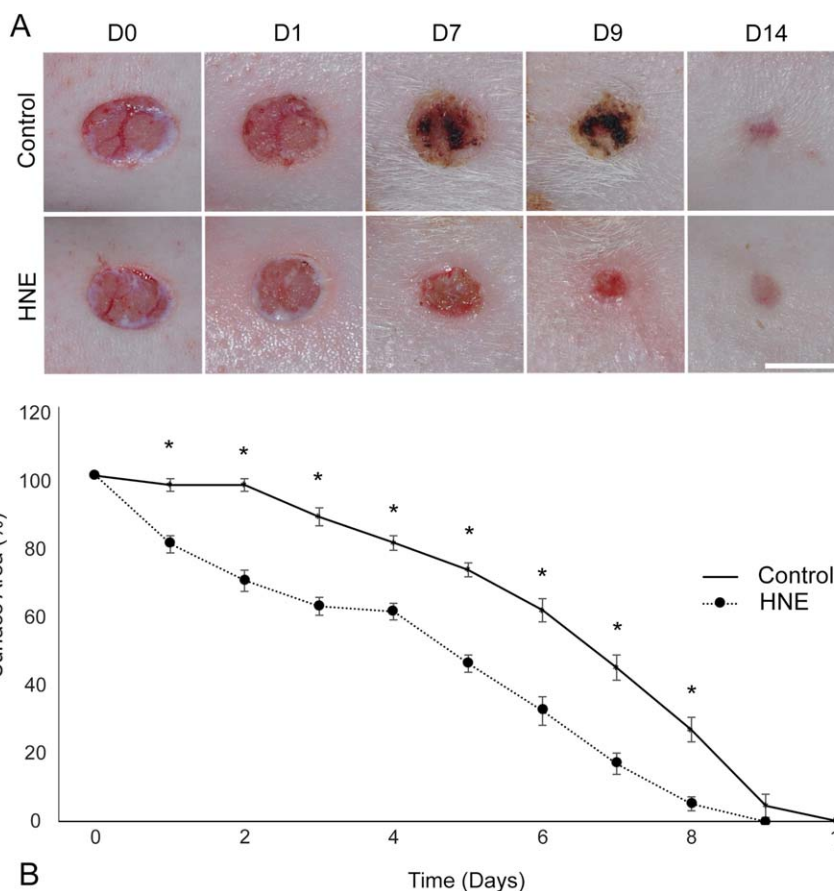
Figure 1. (A) Representative images of noninfected full-thickness dermal injuries treated with wet-to-dry dressings (control) or the hyperosmotic nanoemulsion (HNE). Scale: 8 mm. (B) Measurement of wound closure as a function of time. HNE significantly accelerated time to complete closure, requiring 8.4 ± 0.2 (SEM) days to heal, while control required 9.2 ± 0.2 days for complete closure ($*p < 0.001$). [Color figure can be viewed in the online issue, which is available at wileyonlinelibrary.com.]

indicate position between green and red ($\pm a*$) and yellow and blue ($\pm b*$).[15] The luminosity value of $L* = 0$ corresponds to black with $L* = 100$ representing white. Values toward $+a*$ indicate red while negative values toward $-a*$ indicate green. Similarly, a direction toward $+b*$ indicate yellow while negative values indicate blue. Both $a*$ and $b*$ coordinates range from -127 to $+128$. Shifts in the luminance and chromaticity were recorded during bandage changes for the first 3 days of treatment.

Bacterial contamination quantitation

Microbial contamination for infected animals was conducted via a modified lavage method. Twenty-four hours postsurgery, wound fluid samples were obtained by pipetting 50 μL of sterile saline into the wound bed. The saline solution was then used to lavage the wound and then removed with the pipette. The eluent was then serially diluted and plated onto 10 cm Mueller–Hinton II plates. After 18 h culture at 37 °C, colonies were subjected to quantification and identification. Quantification was done by manual counting. Identification of specific strains of was accomplished using a pathogen recognition technique called BARDOT (bacteria rapid detection using optical scattering technology) that relies on forward-scatter phenotyping.[16,17] Briefly, BARDOT exposes individual bacterial colonies on the agar plate to laser light and then collects

the elastically scattered light pattern (i.e., scattergram) using a CCD camera. These scattergrams were analyzed using Zernike moment invariants and principle component analysis and compared to scattergrams of known bacteria. In this experiment, scattergrams of the reference *E. coli* and *E. faecalis* bacteria were first obtained for 18 h culture time in Mueller–Hinton II agar and digitally stored. Scattergrams from the collected samples (serially diluted) were then compared to the reference library and classified according to their geometric features.[16,17] Colonies outside of the confidence interval to the reference strains were characterized as "other."

Wound bed topography

Surface topography of wounds was assessed with close-range photogrammetry. After euthanization, a thin coating of petroleum jelly was brushed onto the wounds. Next, a model cast of the wound was created with a two-part polyurethane resin mix. Multiple high-resolution images of the plastic model were captured using a DSLR camera with a 1:1 macro lens. Photographs were then processed with reconstructive software (PhotoModeler, Vancouver, BC, Canada) in the automated mode using nontarget feature points to create a 3D topographical reconstruction.
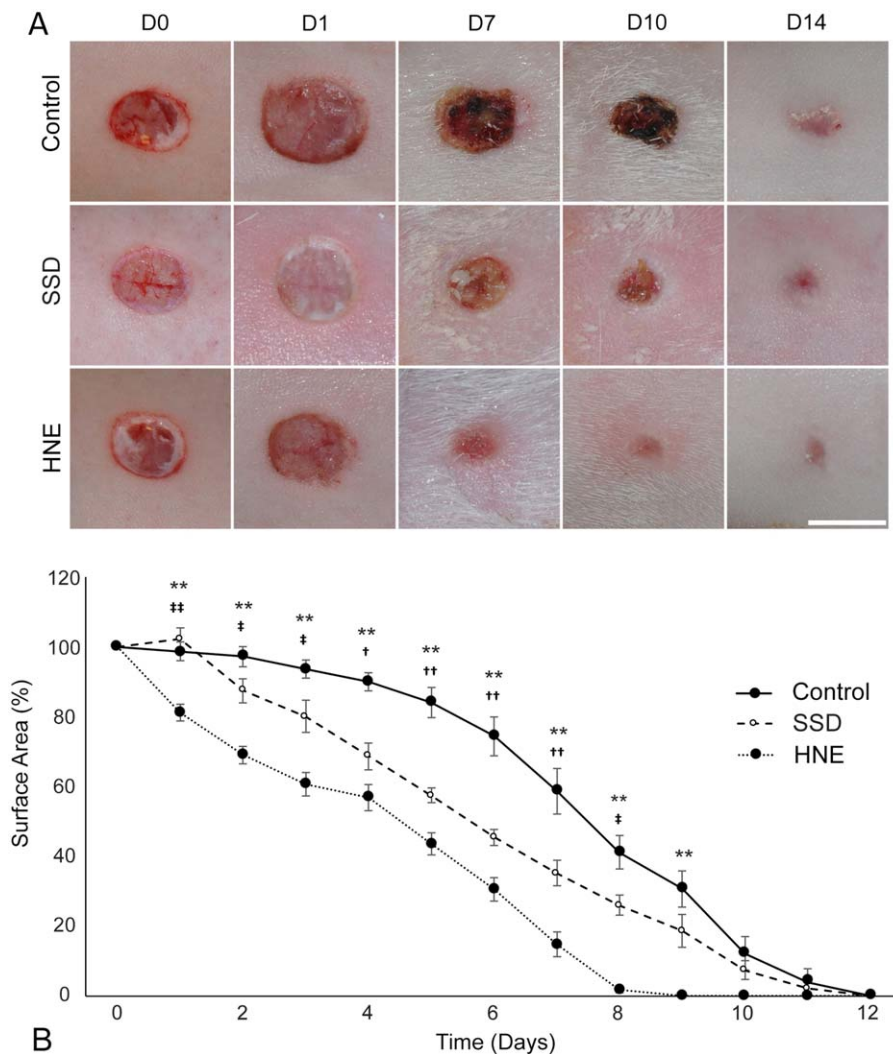
Figure 2. (A) Representative images of infected full-thickness dermal injuries treated with wet-to-dry dressings (control), silver sulfadiazine (SSD), or the hyperosmotic nanoemulsion gel (HNE). Scale: 8 mm. (B) HNE significantly accelerated time to complete closure, requiring 7.6 ± 0.2 (SEM) days to heal, while silver required 10.2 ± 0.4 days and control required 10.4 ± 0.3 days for complete closure. * demarcates significance between control and treatment, † denotes significance between control and silver, and ‡ conveys significance between silver and treatment at $p < 0.05$. Two symbols represent significance at $p < 0.001$, respectively. [Color figure can be viewed in the online issue, which is available at wileyonlinelibrary.com.]

Histology

At designated time points of (2, 7, and 14 days), animals were sacrificed and the tissue processed for histological examination. Tissues were formalin-fixed, paraffin-embedded, cut to 3 μm thickness, and stained with hematoxylin and eosin (H&E) for histologic examination. Tissue sections were also gram stained (MacCallum–Goodpasture Tissue Gram stain).[18] A blinded board certified veterinary pathologist using a modified histomorphologic grading scale presented in Figure 6. Criterion included reepithelialization epidermal hyperplasia, dermal separation, presence of inflammatory cells, adnexal structures, collagenization, fibroblast proliferation and organization, neovascularization, and hemorrhaging. Fibroblast infiltration and proliferation parallel to the wound bed characterize mature granulation tissue. Small-caliber lumen, plump endothelial cells, and perivascular space suggesting leakage of serum distinguish neovascularization morphologically. The maximum obtainable score was 16 (normal skin). In addition, slides at day 14 were imaged and the dermal thickness measured digitally. The dermal thickness served as an indicator of granulation tissue thickness. Measurements were first taken from the surrounding uninjured skin (two averaged measurements) which served as the baseline thickness. Next, the dermal thickness, as measured from the top of the epithelium to the muscle layer, at the wound cross-section midpoint was used. Normalized dermal thickness was taken to be injured/uninjured thickness.

Statistical analysis

Unless noted, all data are reported in the form of AVG $\pm$ SD. Statistical analysis was conducted using a one-way ANOVA and a repeated measures ANOVA for longitudinal wound data. A log-transformation was employed for data involving bacteria. The Tukey post hoc test was used for post hoc evaluation. In all cases, a p value of < 0.05 was considered significant.
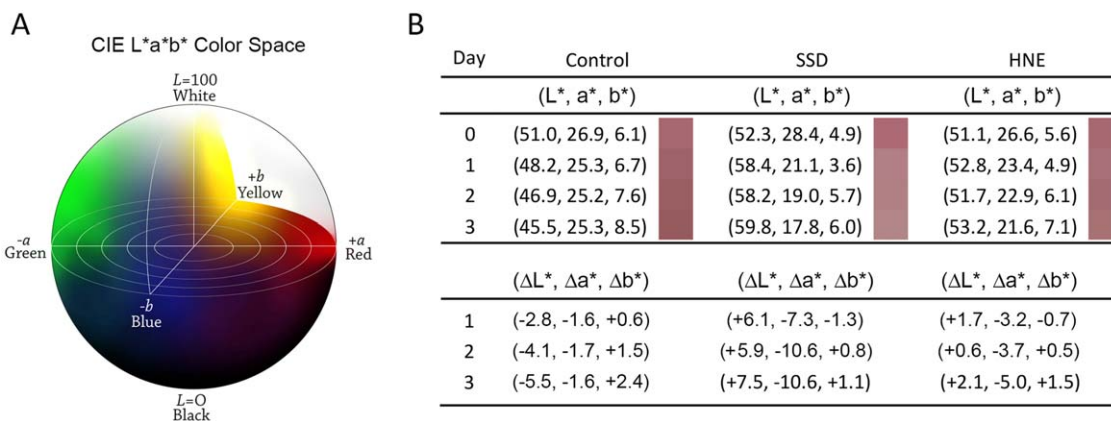
Figure 3. (A) Wound bed color was recorded with a chroma meter and reported in the CIELAB color space, represented by luminosity (L^*) and color direction (a^*, b^*). Luminosity gives the relative brightness ranging from black ($L^* = 0$) to white ($L^* = 100$). Color direction gives the relative hue ranging from red to green ($+a^*$ to $-a^*$, respectively) and yellow to blue ($+b^*$ and $-b^*$, respectively). (B) Color values and wound color progression as a function of treatment.

RESULTS

Wound planimetry

The first experimental group of noninfected cohorts served to demonstrate baseline healing of a standard full-thickness wound. Representative images of treated wounds and rate of healing are shown in Figure 1. When compared to controls, the HNE groups demonstrated significantly faster wound closure. After 8 days of treatment, the wound area in control injuries was reduced by $73.43 \pm 3.63\%$ (SEM)

and HNE treated injuries by $94.92 \pm 1.96\%$. Overall, control injuries required 9.22 ± 0.15 days for complete closure while HNE treated injuries required 8.44 ± 0.24 days to close. The rate of wound closure and corresponding photographs for wounds infected with *E. coli* and *E. faecalis*, are shown in Figure 2. Microbial contamination significantly impaired early stage wound closure in the control treated injuries. The overall size of some wounds increased, as much as 14.29% in a number of control cases on day 1 following surgery. In comparison, SSD-treated wounds did not initially enlarge, but ultimately prolonged
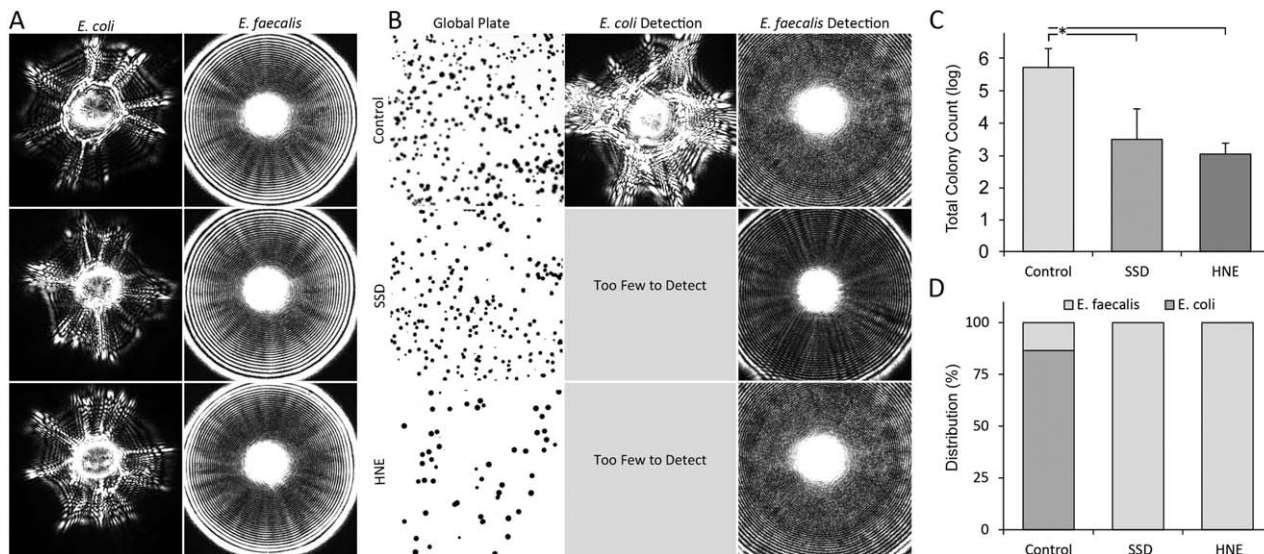

Figure 4. Microbial contamination was measured by plating dilutions and counting colonies using the BARDOT forward light scattering identification system. (A) Reference scattergrams of *E. coli* and *E. faecalis* illustrating reproducible scattered light patterns used to identify recovered wound pathogens. (B) Left: representative images of scanned global plates used for forward light scattering identification. Middle and right: scattergram analysis of as a function of treatment group after 24 h. (C) Total colony counts of wound surface isolates following 24 h of treatment and (D) colony distribution of the microbial population as a function of treatment.
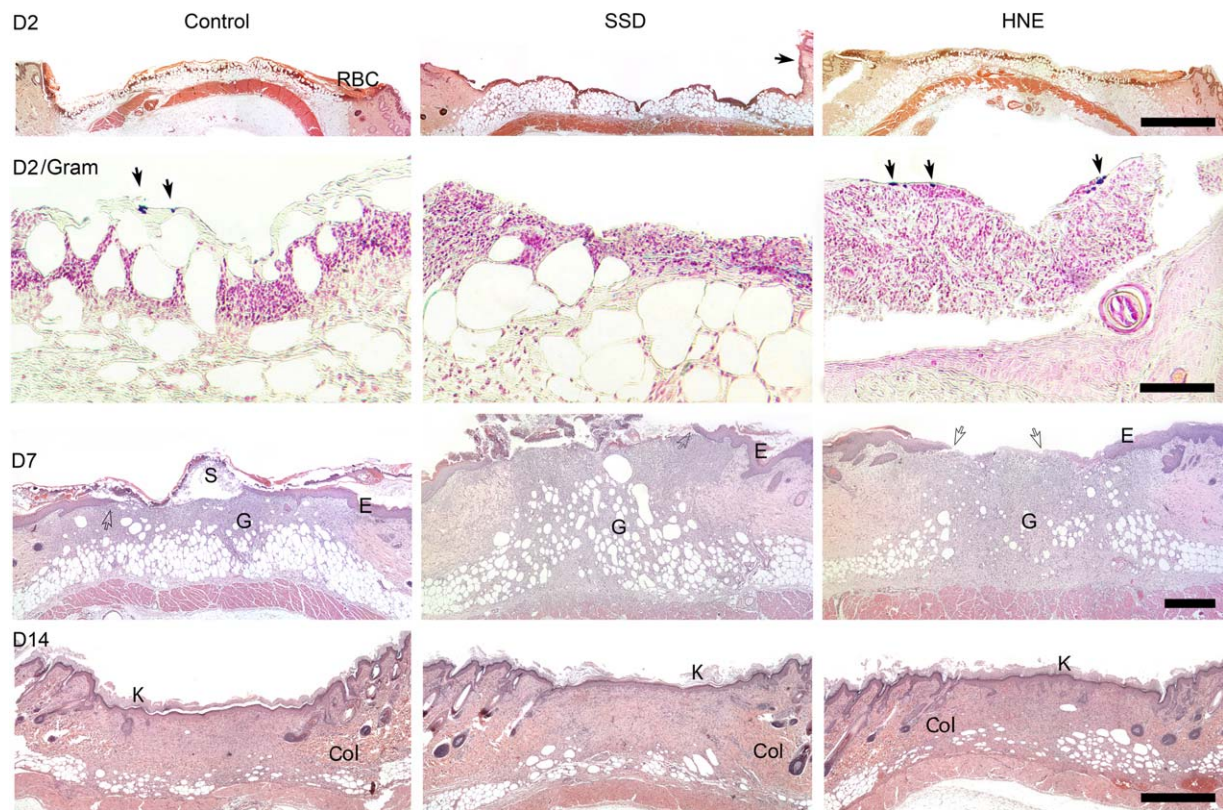
Figure 5. Histological sections taken from representative guinea pig skin samples at 2, 7, and 14 days. Each column represents the treatment groups with H&E staining, with gram staining at day 2 (second row). At 2 days, a large number of red blood cells (RBC) were present in the control wound, whereas in SSD cases, necrotic cells can be observed (black arrow). Scale: 2 mm. Higher magnification gram staining showed some minor aggregates of superficial bacteria in control and HNE (black arrows), but no signs of deeper bacterial residence. Scale: 100 μm. By day 7, (E) reepithelialization and (G) granulation tissue were evident. In the control group, a hard scab (S) had formed in most cases. Open arrows depict the leading edge of epithelium. Scale: 500 μm. At day 14, all wounds were reepithelialized with collagen fibrils present (Col). A keratinized layer (K) can also be found in all cases. Scale: 1 mm. [Color figure can be viewed in the online issue, which is available at wileyonlinelibrary.com.]

healing by inhibiting final attempts to reepithelialize. After 8 days of treatment, control injuries had reduced in size by $59.86 \pm 4.91\%$ and SSD-treated injuries had reduced by $76.61 \pm 2.55\%$. HNE produced the greatest reduction in area with a $99.22 \pm 0.78\%$ decrease after 8 days of treatment. Control injuries required 10.4 ± 0.3 days and SSD-treated injuries required 10.2 ± 0.4 days for complete closure. Conversely, HNE-treated injuries healed significantly faster, requiring only 7.6 ± 0.2 days to heal.

Wound bed color

Wound bed color results shown in Figure 3 are reported in the CIELAB color space and represented by luminosity (L^*) and color direction (a^*, b^*).[15] Control-treated injuries demonstrated a continuous reduction in luminosity ($L^* = -\Delta5.5$) and a slight shift toward an orange–red ($\Delta a^* = -1.6$, $\Delta b^* = 2.4$) after 3 days. Color trends were consistent with macroscopic observation (Figure 2) as the control-treated injuries appeared dark red and formed a thick black scab in the days following insult. SSD-treated wounds demonstrated a rapid increase in luminosity

($L^* = +\Delta7.5$) and transition away from red ($\Delta a^* = -10.6$, $\Delta b^* = 1.1$). The color values correspond to observation as SSD-treated wounds appeared white and did not develop a scab. However, the pale white color was potentially a result of the white excipient base of the SSD cream. Finally, HNE-treated wounds expressed an increase in luminosity ($L^* = +\Delta2.1$) and a significant chromaticity shift toward green ($\Delta a^* = -5.0$, $\Delta b^* = 1.5$). Representative images of HNE-treated wounds confirm color observations, illustrating a light pink wound with limited scab formation through the course of the study.

Bacterial counts

Wound bed contamination was evaluated by vigorous lavaging of the wounds and recovering the fluid for colony enumeration. Samples were serially diluted and cultured to quantify the level of contamination and distribution of strains. Pathogen identification was accomplished using BARDOT, forward-scattering phenotyping.[16,17] Reference scattergrams, shown in Figure 4A, were used to identify microbial strains isolated from the wound bed. Representative cultures

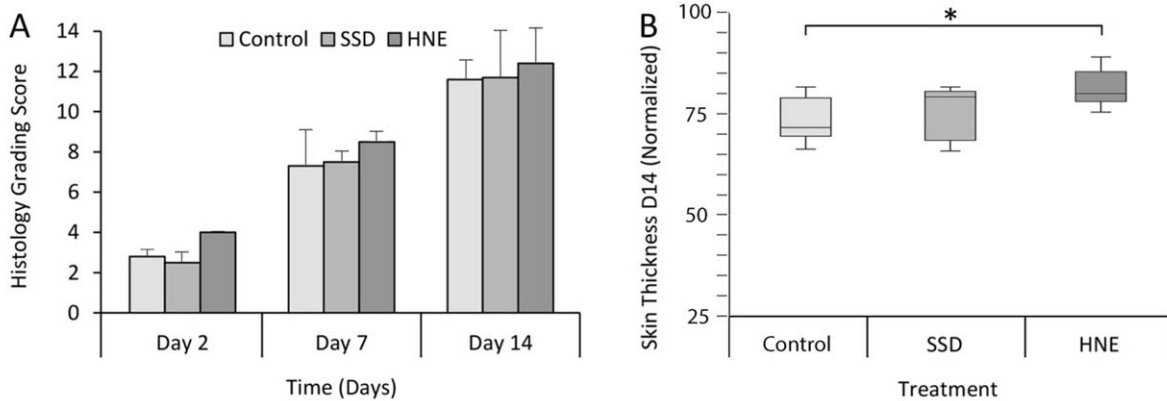| Criterion	Score	Description	Criterion	Score	Description
Re-epithelialization	0	Absent	Collagenization	0	Abnormal lower reticular dermis
	1	<50% intact epidermis		1	Abnormal upper reticular dermis
	2	>50% intact epidermis		2	Abnormal papillary dermis
	3	Intact epidermis		3	Normal dermis
Epidermal Hyperplasia	0	Absent	Fibroblast Proliferation	0	Absent
	1	Present		1	Haphazard arrangement
Dermal Separation	0	Absent		2	Parallel to epithelial surface
	1	Present		3	Normal fibroblasts
Inflammatory Cells	0	Absent	Vascular Proliferation	0	Absent
	1	Present		1	Present
Adnexal Structures	0	Absent	Hemorrhage	0	Present
	1	<100% present		1	Absent
	2	Present and normal			

Figure 6. Histological assessment of tissue extracts at days 2, 7, and 14. (A) Histology score ($\pm$SD) based on the criterion outlined in above table for each treatment methodology. (B) Box plot of dermal thickness measurements acquired at day 14. Results were normalized to uninjured control tissue for comparison (*$p < 0.05$). [Color figure can be viewed in the online issue, which is available at wileyonlinelibrary.com.]

acquired from the wound bed are shown in Figure 4B. Results show a significant reduction in bacteria colony forming units for SSD- and HNE-treated wounds in comparison to the control (Figure 4C). Control injuries were found to have approximately 5.4×10^5 CFU 24 h postinoculation, whereas 2.6×10^3 CFU were recovered from SSD-treated sites. Similarly, 3.15×10^3 CFU were found in the HNE-exposed wounds, representing a 2.5 log reduction in CFU compared to control. BARDOT was performed on the culture dishes, which identified *E. coli* and *E. faecalis* in the control samples but only *E. faecalis* in the SSD and HNE treatment groups. (Figure 5D). No other bacterial strains were detected on a consistent basis.

Histology

Histological sections (Figure 5) of the harvested tissue at days 2, 7, and 14 further corroborate the macroscopic results. Samples for the gauze control at Day 2 demonstrated hemorrhaging as shown by the extravasated red blood cells at the wound surface and a mixture of neutrophils and macrophages. The inflammatory cells are an expected component of normal wound healing to clean up debris of damaged cells. In contrast, both SSD and HNE showed less hemorrhage at day 2 but SSD had more

necrosis in the superficial stratum spinosum of the epidermis. Gram staining of slides on day 2 showed no significant bacteria penetration into the tissue. However, small aggregates of bacteria were observed superficially in the HNE and control samples. Most of these aggregates were isolated, with few being above the newly formed epithelium. By day 7, the wounds were histologically similar but the gauze controls were marked with a thick scab of exudate and cellular debris. Reepithelialization from the margins was observed in all wound groups at day 7. Granulation tissue was also evident. At day 14, all wounds were completely reepithelialized. Cumulative histological scores using the grading criteria (Figure 6) depict the largest differences within the first week of healing. However, measurements of dermal thickness show the control wounds were thinner with less granulation tissue present on day 14. Control wounds were $73.9 \pm 5.1\%$ of the normal thickness, whereas HNE and SSD were $81.0 \pm 4.7\%$ and $76.4 \pm 7.4\%$, respectively (Figure 6B).

Wound bed topography

Later stages of wound closure were evaluated by monitoring tissue remodeling using close-range photogrammetry. Images of the wound bed at day 14 were used to
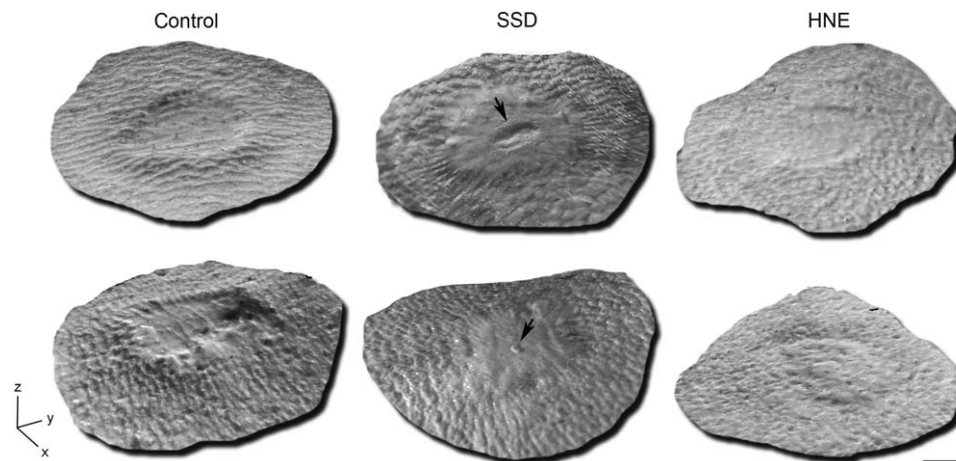
Figure 7. Representative close-range 3D photogrammetry of control, SSD, and HNE-treated wounds from the infected cohort after 14 days. In the SSD treatments, incomplete reepithelialization was observed in some instances and manifested as minor depressions in the central wound region (black arrows). Scale: 2 mm.

reconstruct the 3D geometry of the lesion for topographical assessment. Representative models are shown in Figure 7. Analysis revealed that HNE-treated wounds produced a much smoother surface and more complete tissue fill in comparison to either the untreated control or SSD treated. In several cases of SSD, a small craterous region in the wound center was observed.

DISCUSSION

Hyperosmotic agents, including simple sugars and honeys, have been described in ancient Egyptian texts for applications in wound management. Formal clinical evidence for the use of ordinary table sugar in wounds was first presented in series of case studies by Herszage.[19] Treatment with granulated sugar indicated a 99.2% success rate across various wound etiologies with complete wound closure within 9 days to 17 weeks. The authors observed that wound odor and secretion drastically reduced by 24–96 h following sugar application. Further, Knutson et al. conducted clinical trials using a mixture of granulated sugar and povidine–iodine to treat infected burns and ulcers.[20,21] Key findings from the report indicated sugar treatment reduced bacterial contamination, debrided eschar, and promoted granulation tissue.

Historical studies suggest hyperosmotic agents exert their action via a couple of mechanisms: (i) the hygroscopic action of the sugars help maintain a moist wound environment and increase tissue microcirculation; and (ii) the sugars inhibit microbial growth by presumably lowering the local water activity.[7,22] Other reviews describe sugar treatments may reduce edema and provide an acidic pH that favors wound healing.[5] Despite promising attributes, sugars alone are bacteriostatic as microbes can adapt to hyperosmotic stress. For example, in response to hypertonicity, bacteria can decrease membrane fluidity by altering phospholipid composition and/or accumulate compatible solutes (i.e., K^+ ions, specific amino acids, quaternary amines, and the sugars) either through de novo synthesis or by active transport

to offset the extracellular solute concentration.[10,23] This adaptive machinery allows many bacteria strains to remain viable even at osmolarities near the solubility limit of the applied solutes.[9,10] In the case of honey, additional antimicrobial agents may be present, such as peroxides and non-peroxide compounds.[24] However, the concentration of these chemical species varies widely with honey type and origin.[25,26]

Accordingly, our rationale was to develop a hyperosmotic-based treatment that retained the positive wound healing benefits of sugars while providing controlled antimicrobial properties. We previously demonstrated that disrupting the bacterial cell membrane impaired microbial adaptation to even mild shifts in osmotic stress.[11] Combining membrane-disrupting nanoemulsions with hyperosmotic sugars (HNE) synergistically facilitated the efflux of intracellular water, K^+, and nucleic acids across the compromised bacterial membrane. The broad-spectrum bactericidal action occurred in a timeframe of a minute or less in vitro.[11]

The purpose of this study was to further explore HNE as topical antimicrobial. We first assessed the effects of HNE in noncontaminated wounds using a full-thickness dermal injury in guinea pig.[27,28] Results demonstrate that HNE was well tolerated and caused minimal bystander damage. Indeed, in the noninfected pilot cohort, the HNE-treated wounds healed slightly faster than wet to dry bandaged control wounds (8.44 ± 0.24 vs 9.22 ± 0.15 days for total wound closure). The HNE wounds maintained a moist wound environment, whereas the control group tended to form a scab a week after wound creation. No signs of periwound inflammation or adverse reactions were observed with HNE. Based on these results, the HNE dosing and application schedule was kept the same for the remainder of the experiments.

Subsequent studies involved inoculating wounds with a mixture of *E. coli* and *E. faecalis* bacteria at a total of 5×10^6 CFU. Wet-to-dry gauze (control) and SSD/foam combination were used as comparison. These contamination studies showed several differentiating characteristics between treatments. First, the control wounds had a very

slight reduction in the amount of recovered surface bacteria (<1 log) compared to the initial inoculum. In many cases, $>1 \times 10^6$ CFU were recovered from the wounds after 24 h. Analysis of the wound CFU using forward optical light scattering showed the distribution of bacteria to be approximately 75% *E. coli* and 25% *E. faecalis*. In contrast, both SSD and HNE demonstrated bacteria levels ~2.5 logs lower. Only *E. faecalis* was recovered from the SSD- and HNE-treated wounds. Other types of competing microbes were not prevalent in the wound at 24 h. The shift in the wound flora is noteworthy. It may be possible that *E. coli* may be more sensitive to hyperosmotic stress or less adapted to the wound microenvironment compared to *E. faecalis*. Such findings may offer insight into the role of hyperosmotic topicals in treating specific strains in polyflora wounds.

In addition to bacteria enumeration, wound bed color and wound size were used to track healing. Wound color has been used to assess viability of chronic wounds[29] and we have adapted the method to assess inflammation or color changes during healing. Wound bed color data show control wounds got darker (luminance) over time while chromaticity values depict a shift toward red. These brightness and hue shifts for the control are indicative of either inflammation or poor hemostasis and this was confirmed both visually and histologically as many red blood cells were found encrusted on the surface of the control group. The HNE group color did not change significantly while the SSD became less red and brighter. This was due to a bleaching effect between the SSD paste and the underlying tissue.

The primary difference between the treatments, however, was in rate of wound closure. Control wounds often expanded after the first 24 h after wound creation and contamination. This is in contrast to the noncontaminated pilot animals, in which the wounds decreased in size postinjury. Other studies have shown similar findings, in which infected wounds may enlarge prior to contraction.[30] No marked dilation in wounds was found in either SSD or HNE groups and all wounds were fully contracted and similarly epithelialized by day 14. However, at day 14, a thicker granulation layer was found in the HNE cohort vs control as reflected in the dermal thickness measurements. Histologic parameters (Table 1) were scored visually by a blinded pathologist at days 2, 7, and 14. The semiquantitative trends show marked histological improvements such as less hemorrhage in HNE during the first few days after injury. Gram stained tissue at 2 days postsurgery revealed that most of the initial bacteria had been cleared, with some small pockets of superficial bacteria. No signs of deeper bacterial infiltration were found. At days 7 and 14, the differences between treatments tended to converge.

While the HNE treatment improved wound healing, the obtained data also suggest silver may be cytotoxic and delay healing. Others have shown in vitro that the minimal biocidal concentration of silver is sufficient to cause irreparable damage to fibroblasts and keratinocytes.[2] We found that silver caused more necrosis in the apical cell layers at 2 days postinjury. Histologically, SSD also had a poorer hemostatic response compared to HNE with less fibrin present. Bandage removal on days 9–10 showed some wounds were not fully closed and there were small localized areas of bleeding. In comparison, both HNE and control wounds did not exhibit hemorrhage at the same time points. Three-dimensional topographical reconstructions of the wounds displayed a slight depression in the wound epicenter 14 days postinjury, which was coincident with a very thin epithelial layer. The aggregate findings suggest SSD may disrupt or delay the migration of keratinocytes when applied daily.

We hypothesize that the HNE acts similarly to hyperosmotic sugars in which the hygroscopic effect actively draws wound fluids through the wound bed to irrigate, debride, and help maintain a moist wound. This is supported both histologically and macroscopically as depicted by a thin fibrin layer in the HNE group instead of a thick hard scab in the control. The high level of exudate produced by topical HNE should be managed properly, as normal wet–dry bandages caused some maceration in pilot animals (data not shown). Therefore, we recommend the use of highly absorbent dressings in conjunction with hyperosmotic preparations. The nanoemulsion component, in conjunction with hyperosmotic stress, most likely acts as a preservative that further discourages microbial growth in the moist wound environment. While hyperosmotic sugar and honeys have been associated with scar reduction,[31,32] scarring could not be appropriately assessed in this acute timescale. Nonetheless, the 3D topographical reconstructions of wounds corroborate enhanced granulation tissue formation and improved wound fill vs control. We speculate these characteristics may potentially decrease the appearance of scarring. Finally, dermal sensitization and irritation studies in rabbit and guinea pigs did not reveal any side effects from HNE as the treatment received the lowest observable score of 0 in these tests (Supporting Information, A1). As a result, the applied HNE dose does not appear to induce sensitization or acute dermal irritation.

Future studies concerning the dose response of HNE are warranted. For example, we currently used a low concentration of thymol by weight, but higher concentrations may possess improved antimicrobial activity. Additionally, other wound modalities, including partial thickness injuries, burns, and chronic wounds may benefit from the hyperosmotic treatments. In conclusion, HNE improved granulation tissue formation and wound closure in both noninfected and contaminated wounds. No adverse reactions were seen. Based on these findings, hyperosmotic emulsion treatments may have potential in the management of acute wounds.

ACKNOWLEDGMENTS

REFERENCES

1. Warriner R, Burrell R. Infection and the chronic wound: a focus on silver. *Adv Skin Wound Care* 2005; 18 (Suppl 1): 2–12.

2. Poon VK, Burd A. In vitro cytotoxity of silver: implication for clinical wound care. *Burns J Int Soc Burn Injuries* 2004; 30 (2): 140–7.

3. Burd A, Kwok CH, Hung SC, Chan HS, Gu H, Lam WK, *et al*. A comparative study of the cytotoxicity of silver-based dressings in monolayer cell, tissue explant, and animal models. *Wound Rep Regen* 2007; 15 (1): 94–104.

4. Hollinger MA. Toxicological aspects of topical silver pharmaceuticals. *Crit Rev Toxicol* 1996; 26 (3): 255–60.

5. Biswas A. bM, Hurst C, Gruessner R, Armstrong D, Rilo H. Use of sugar on the healing of diabetic ulcers: a review. *J Diabet Sci Technol* 2010; 4 (5): 1139–45.

6. Vaara M. Agents that increase the permeability of the outer-membrane. *Microbiol Rev* 1992; 56 (3): 395–411.

7. Chirife J, Herszage L. Sugar for infected wounds. *Lancet* 1982; 2 (8290): 157.

8. Middleton K. Sugar paste in wound management. *Dressing Times* 1990; 3 (2): 22.

9. Carpita NC. Tensile-strength of cell-walls of living cells. *Plant Physiol* 1985; 79 (2): 485–8.

10. Csonka LN. Physiological and genetic responses of bacteria to osmotic stress. *Microbiol Rev* 1989; 53 (1): 121–47.

11. Connell S, Li JM, Shi RY. Synergistic bactericidal activity between hyperosmotic stress and membrane-disrupting nanoemulsions. *J Med Microbiol* 2013; 62 (1): 69–77.

12. Hammond CE, Nixon MA. The reliability of a handheld wound measurement and documentation device in clinical practice. *J Wound Ostomy Cont* 2011; 38 (3): 260–4.

13. Rogers L, Bevilacqua N, Armstrong D, Andros G. Digital planimetry results in more accurate wound measurements: a comparison to standard ruler measurements. *J Diabet Sci Technol* 2010; 4 (4): 799–802.

14. Little C, McDonald J, Jenkins M, McCarron P. An overview of techniques used to measure wound volume and area. *J Wound Care* 2009; 18 (20): 250–3.

15. Romanelli M, Gaggio G, Coluccia M, Rizzello F, Piaggesi A. Technological advances in wound bed measurements. *Wounds* 2002; 14 (2): 58–66.

16. Rajwa B, Dundar MM, Akova F, Bettasso A, Patsekin V, Hirleman ED, *et al*. Discovering the unknown: detection of emerging pathogens using a label-free light-scattering system. *Cytom Part A* 2010; 77A (12): 1103–12.

17. Banada PP, Guo SL, Bayraktar B, Bae E, Rajwa B, Robinson JP, *et al*. Optical forward-scattering for detection of Listeria monocytogenes and other Listeria species. *Biosens Bioelectron* 2007; 22 (8): 1664–71.

18. Luna LG Jr. *Manual of histologic staining methods of the Armed Forces Institute of Pathology*. New York: McGraw-Hill Book Company, 1968.

19. Herszage L, Montenegro JR. Sugar for infected wounds. *Gaz Med-France* 1984; 91 (31): 59.

20. Knutson RA. Accelerated wound and burn healing using sugar and povidone-iodine. *Southern Med J* 1983; 76 (9): P35–P3P.

21. Knutson RA, Merbitz LA, Creekmore MA, Snipes HG. Use of sugar and povidone–iodine to enhance wound-healing - 5 years experience. *Southern Med J* 1981; 74 (11): 1329–35.

22. Chirife J, Herszage L, Joseph A, Kohn ES. In vitro study of bacterial-growth inhibition in concentrated sugar solutions - microbiological basis for the use of sugar in treating infected wounds. *Antimicrob Agents Chemother* 1983; 23 (5): 766–73.

23. Csonka LN, Hanson AD. Prokaryotic osmoregulation - genetics and physiology. *Ann Rev Microbiol* 1991; 45: 569–606.

24. Mavric E, Wittmann S, Barth G, Henle T. Identification and quantification of methylglyoxal as the dominant antibacterial constituent of Manuka (Leptospermum scoparium) honeys from New Zealand. *Mol Nutr Food Res* 2008; 52 (4): 483–9.

25. Leon-Ruiz V, Gonzalez-Porto AV, Al-Habsi N, Vera S, San Andres MP, Jauregi P. Antioxidant, antibacterial and ACE-inhibitory activity of four monofloral honeys in relation to their chemical composition. *Food Funct* 2013; 4 (11): 1617–24.

26. Ahmed S, Othman NH. Review of the medicinal effects of tualang honey and a comparison with manuka honey. *Malay J Med Sci MJMS* 2013; 20 (3): 6–13.

27. Dai TH, Kharkwal GB, Tanaka M, Huang YY, de Arce VJB, Hamblin MR. Animal models of external traumatic wound infections. *Virulence* 2011; 2 (4): 296–315.

28. Davidson J. Animal models for wound repair. *Arch Dermatol Res* 1998; 290 (1): S1–11.

29. Romanelli M. Objective measurement of venous ulcer debridement and granulation with a skin color reflectance analyser. *Wounds* 1997; 9 (4): 122–6.

30. Burkatovskaya M, Castano AP, Demidova-Rice TN, Tegos GP, Hamblin MR. Effect of chitosan acetate bandage on wound healing in infected and noninfected wounds in mice. *Wound Rep Regen* 2008; 16 (3): 425–31.

31. Topham J. Sugar for wounds. *J Tissue Viab* 2000; 10 (3): 86–9.

32. Molan PC. Re-introducing honey in the management of wounds and ulcers - theory and practice. *Ostomy/Wound Manage* 2002; 48 (11): 28–40.

Supporting Information

Additional Supporting Information may be found in the online version of this article.